CHAOS IN 2D SLOW-FAST MAPS FOR SPIKING-BURSTING NEURAL ACTIVITY

Andrey Shilnikov

Department of Mathematics and Statistics,
Georgia State University, Atlanta, GA 30303, USA
e-mail: ashilnikov@mathtat.gsu.edu
WWW: http://www.mathstat.gsu.edu/matals

Nikolai Rulkov

Institute for Nonlinear Science,
University of California at San Diego, La Jolla, CA 92093, USA
e-mail: nrulkov@ucsd.edu
WWW: http://http://inls.ucsd.edu/ rulkov

Abstract— *Origin of chaos in a simple slow-fast 2D map replicating the spiking and spiking-bursting activity of real biological neurons is studied. The map contains one fast and one slow variable. We study the bifurcation scenarios which reveal the dynamical mechanisms that lead to chaos through canards in alternation of silence and spiking phases.*

I. Introduction

Spiking-bursting activity of biological neurons is the result of high-dimensional dynamics given by nonlinear dynamical processes of generation and interaction of various ionic currents flowing through the membrane channels of each neuron [7]. Numerical studies of such neural activity are usually based on either realistic channel-based models or phenomenological models. The channel-based models proposed for a single neuron are designed to capture the physiological processes in the membrane. These models are usually given by a system of many nonlinear differential equations. Recently a similar type of phenomenological models, but based on a low-dimensional map, was proposed. The interest in the map models is motivated by the studies of nonlinear mechanisms behind the restructuring of the collective neural behavior in large networks. Here we consider a map model which is built following to the principles for constructing a low-dimensional system of differential equation which is capable of generating fast spikes bursts excited on top of the slow oscillations (see for example [6], [11], [2], [8]). These two time-scale oscillations are captured using a system with both slow and fast dynamics. In the case of map, such a system can be designed in the following form [12]

$$x_{n+1} = f(x_n, y_n)\ , \quad y_{n+1} = y_n - \mu(x_n + 1 - \sigma), \tag{1a}$$

where x_n is the fast and y_n is the slow dynamical variable as $|\mu| \ll 1$. The parameter σ is a control parameter which is used to select the regime of individual behavior. The fast map is built to mimic spiking

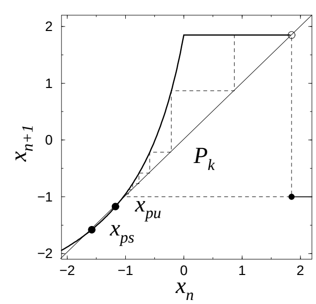

Fig. 1. Dynamics of fast map computed with $\alpha = 5.6$ and fixed value of $y_n = y = -3.75$. The stable and unstable fixed points of the map are indicated by x_{ps} and x_{pu}, respectively.

and silent regimes. This is achieved with the use of discontinuous function $f(x, y)$ of the following form

$$f(x,y) = \begin{cases} \alpha/(1-x) + y, & x \le 0 \\ \alpha + y, & 0 < x < \alpha + y \\ -1, & x \ge \alpha + y \end{cases} \tag{2}$$

where α is a control parameter of the map.

Typical regimes of temporal behavior of the two-dimensional map are shown in Fig 2. It was shown in [12] that using approximate analysis of fast and slow dynamics one can explain the regimes of silence,

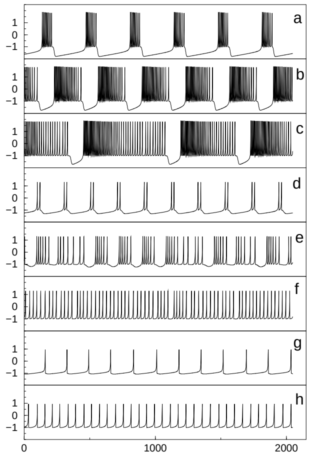

Fig. 2. Typical waveforms of spiking and spiking-bursting behavior generated by the map computed for the following parameter values: **(a)** $\alpha = 5.6$, $\sigma = -0.25$; **(b)** $\alpha = 5.6$, $\sigma = 0.2$; **(c)** $\alpha = 5.6$, $\sigma = 0.322$; **(d)** $\alpha = 4.6$, $\sigma = -0.1$; **(e)** $\alpha = 4.6$, $\sigma = 0.16$; **(f)** $\alpha = 4.6$, $\sigma = 0.225$; **(g)** $\alpha = 3.9$, $\sigma = 0.04$; **(h)** $\alpha = 3.9$, $\sigma = 0.15$. The points of the consecutive iterations x_n are connected with straight lines.

continuous spiking, and the generation of the bursts of spikes occurred in the map (1). However such analysis does not explain the dynamical mechanism behind the chaotic spiking and chaotic spiking-bursting behaviors. Understanding of the origin of a chaotic behavior in the map is the focus of the given study.

A. Local Bifurcation of the Fixed Point

We restrict our consideration to the rectangular $\{2 \leq a \leq 8;\ -2 \leq \sigma < 1\}$. Here 1) has a single fixed point $O(x_o = -1+\sigma, y_o = x_o - \frac{\alpha}{1-x_o}$. The Jacobian matrix $\mathbf{J}$ of the map at the fixed point is given by $\mathbf{J} = \begin{pmatrix} \frac{\alpha}{(2-\sigma)^2} & 1 \\ -\mu & 1 \end{pmatrix}$. In the case of the Andronov-Hopf (AH) bifurcation for maps the Jacobian and the trace of $\mathbf{J}$ become 1 and $2\cos\psi$, respectively. Then one can find the equation of bifurcation curve AH which is given by $\sigma = 2 - \sqrt{\alpha/(1-\mu)}$. On it the fixed point has the following multipliers: $\rho_{1,2} = \frac{2-\mu}{2} \pm \frac{i}{2}\sqrt{(4-\mu)\mu} = \cos\psi \pm i\sin\psi$. Observe that $\rho_{1,2}$ depend on μ only. The stability of the fixed point on AH is determined by the sign of the first Lyapunov coefficient L_1. The point is stable when $L_1 < 0$ and repelling otherwise. The tedious calculations reveal $L_1 > 0$.

II. Canards and chaotic spiking

At the subcritical Andronov-Hopf bifurcation the fixed point loses its stability when an unstable invariant curve shrinks into it. To complete the picture of qualitative behavior of the map near the threshold we need to examine the evolution of this invariant curve with the parameter change, and answer the question: where does the unstable invariant curve come from? A comprehensive answer to the question on the origin of the invariant curve requests an examination of a special solution known as *a canard* or a French duck. We will call it a Hopf-initiated canard for consistency with the classification proposed in [5].

The mechanism underlying a canard can be reiterated in our case as follows. Consider the curve S_{fp} of slow motions of map (1) at $\mu = 0$. The slow manifold lacks the normal hyperbolicity property near the fold where S_{ps} and S_{pu} merge; this fold is the saddle-node point of the fast map. As follows from [4] that when μ is small the normal hyperbolic pieces of S_{pu} and S_{ps} will persist as some invariant critical manifolds $\mathcal{S}_u$ and $\mathcal{S}_s$, both μ-close to the original branches. As a control parameter of the system varies the manifolds $\mathcal{S}_u$ and $\mathcal{S}_s$ may touch each other, cross (in maps) thereby forming the canard manifold breaking up as they swap over in further. Four snapshots taking the critical manifolds near the fold are shown in Fig. 3 illustrating the evaluation of the canard as σ increases. The first picture shows the stable critical

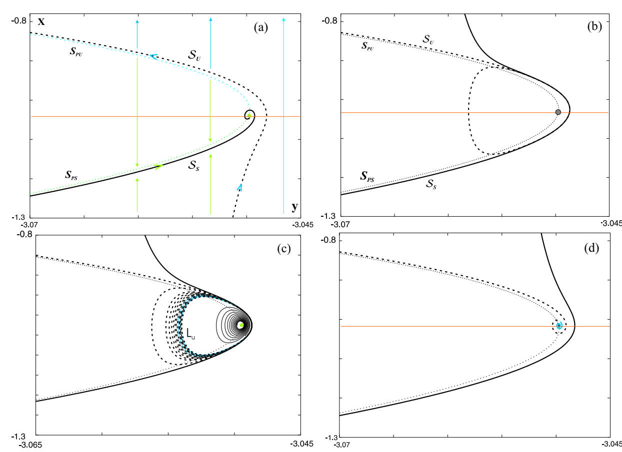

Fig. 3. Stages of canard formation: $\mu = 0.001$ $\alpha = 4.1$ and σ equal to -0.0262 in (a); -0.026113175787 in (b); -0.02605 in (c); and -0.016 in (d). In panel (a) $\mathcal{S}_s$ converges to the stable point whose basin of attraction is determined by $\mathcal{S}_f$. (b) Critical canard manifold and birth of the closed unstable invariant curve. (c) The last bounds the basin of the stable point. (d) The unstable critical manifold spirals out of the fixed point, stable in backward time.

manifold $\mathcal{S}_s$ converging to the attracting fixed point before the Andronov-Hopf bifurcation. The last figure 3(d) shows the unstable invariant manifold $\mathcal{S}_u$ spiraling out of the now unstable fixed point after the bifurcation. When the bifurcation curve AH is crossed leftward, the fixed point becomes stable and its absorbing basin is bounded by the unstable invariant curve L_u. The latter is the α-limit set for the trajectories close to $\mathcal{S}_u$ shown in Figs. 3(c). As σ decreases slightly further the size of L_u increases and at some critical value of σ the critical manifolds $\mathcal{S}_s$ and $\mathcal{S}_u$ touch or cross each other, see Fig. 3(b) . As they swap over each other, the invariant curve L_u vanishes, see Figs. 3(a).

When the critical manifold $\mathcal{S}_S$ moves further in parallel to $\mathcal{S}_U$ a neighboring trajectory will be dragged along with it into the unstable region. Such a solution is called a *canard*. The canard solutions are characterized by a high sensitivity to initial conditions which is due to the blowing instability near the unstable critical manifold that separates and repels the nearby trajectories on both sides in opposite directions. When this instability lifts a trajectory up off the unstable critical line, it is mirrored by the limiter built in the function (2) downwards throughout line $x = -1$ towards stable critical manifold $\mathcal{S}_S$, along which the trajectory slides slowly to the right. Two distinct phase portraits reflecting this situation are shown in Fig. 4. Figure 4(a) illustrates the regime of bi-stability where the canard initiated chaos coexists with the stable fixed point whose local absorbing basin is surrounded by the unstable invariant closed curve L_u. Here, the beam of the the phase trajectories first widens along the canard and then gets split and mixed at the point $(x = 0, y = \alpha)$ gluing the two piece-wise continuous segments of nonlinear function (2) of the map (1). The chaotic attractor shown in Fig. 4(a) is the image of the continuous spiking characterized by irregular inter-spike-intervals. As one can see from this figure this type of spiking activity can coexist with the silence mode when the map is close enough to the threshold of excitation.

A. Chaotic bursting

Here we consider the soft transition from the regime of continuous spiking to the bursting activity that occurs within a wedge-shaped border originating from the threshold $(\alpha = 4; \sigma = 0)$. The mechanism of this transition in the case of finite values of μ is illustrated in Fig. 5. Green trajectory, whose initial point is chosen by the stable critical manifold $\mathcal{S}_s$, tends to the attractive ω-limit set. One can see that the map generates continuous spikes when the attractor is such as shown in Fig 5(a). In contrast, Figure 5(b) illustrates the regime of bursts. Here a burst means that the continuous spiking phase is altered by relatively long interval of silence while the trajectory drifts along the stable critical manifold.

Consider the evolution of the shape of the attractor on the path $(\alpha = 5; \sigma = 0.3 \to 0.28)$. Fig 5a is taken at $\sigma = 0.3$. At this moment the stable critical manifold $\mathcal{S}_s$ makes a first touch with the unstable critical one $\mathcal{S}_u$ at some point on the line $x = -1$. This situation is very similar to the canard formation discussed above. As then, the phase point can be dragged along the unstable critical manifold which results in a spontaneous jump up or down. This leads to high sensitivity of the trajectories behavior on initial conditions and brings a chaotic component into the dynamics of bursts. As σ decreases further the attractor descends below $\mathcal{S}_u$ so that the phase point starts making the straight jumps down onto the stable critical manifold, thereby forming a genuine burst in Fig. 5b. The number of the spikes in a burst can be constant or alternating depending on how close the attractor is

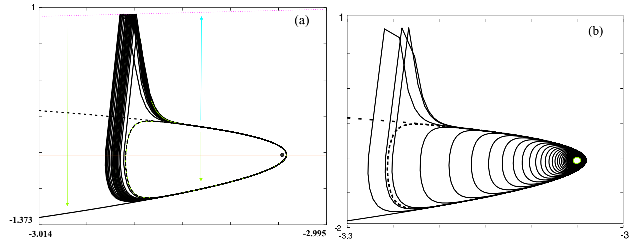

Fig. 4. (a) Example of instant chaos at $\alpha = 3.995$, $\sigma = 0.0$ and $\mu = 0.001$. Due to spontaneous jumps of the phase point off the canard the number of its iterates as it climbs up the plateau on nonlinear characteristic differs every circulation. (b) The unstable invariant curve does not bounds the "local" attraction basin of the stable fixed point; $\alpha = 4.1$, $\sigma = -0.03445$ and $\mu = 0.00749915834$. By "local" the attraction basin of the stable fixed point of the locally invertible map is understood.

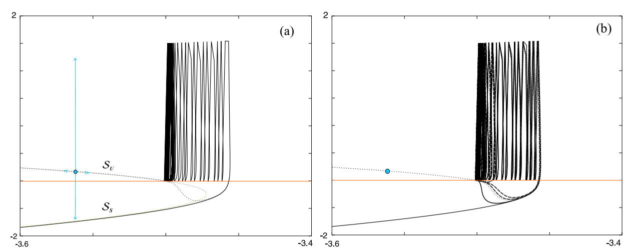

Fig. 5. Transformation of tonic spikes ((a) $\alpha = 5$, $\sigma = 0.3$) into bursts ((b) $\sigma = 0.28$) via the tangency of the stable and unstable sets of the singularly perturbed map. The appendix of the bursts phase grows as the iterates lower below $\mathcal{S}_u$.

to the unstable critical line or, in other words, whether the canard behavior is regular or complex.

Finally we discuss the mechanism of the generation of chaotic bursts through the homoclinic bifurcations of the repelling fixed point of the 2D map (1). Such a bifurcation is one of the features of non-invertible maps [10]. In our case the dimension of the unstable set W^u_O of the repelling fixed point O is two, whereas the stable set W^s_O is null-dimensional. A point $p = W^u_O \cap W^s_O$ is a homoclinic one if its forward and backward iterates converge to the fixed point O. The fixed point is called a snap-back repeller if its small neighborhood contains a homoclinic point whose forward sequence of iterates ending up at the fixed point is finite. The existence of a transverse homoclinic orbit to the repeller implies the existence of a *scrambled set*, introduced by Marotto [9]. The scrambled set is an analog of a hyperbolic subset which is the closure of the transverse homoclinic trajectory in a proper invertible map. It consists of countably many repelling periodic orbits and a continuum of positive Poisson stable trajectories. The presence of such trajectories is a signature of chaos [13]. The snap-back

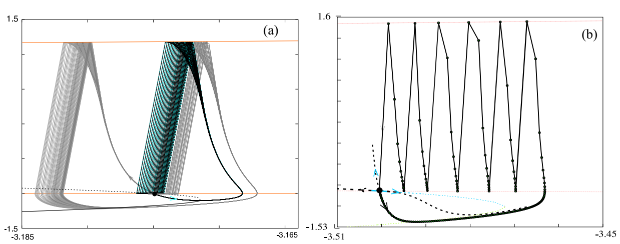

Fig. 6. (a) Primary and secondary homoclinics to the repelling point existing within $[4.3339\,; 4.3679]$ at $\alpha = 4.3499$; (b) shows the six-spike homoclinic orbit turning into a seven-spike one at $\alpha = 5.01$.

bifurcations and, respectively, the homoclinic orbits are distinguished by the number of spikes in a burst, see for example Fig. 6. In particular, Fig. 6a shows the map generating chaotic sequences of the single and the double-pulse bursts.

Another, yet similar, way of waveform transformations is illustrated in Fig. 7 far from the homoclinic bifurcation. As above the core of the mechanism is the interplay between the unstable manifold $\mathcal{S}_u$ and the locus of the attractor. Recall that the direction of the jump — up or down of the phase point landing onto the line $x = -1$ is determined whether the its coordinates are above or below $\mathcal{S}_u$ respectively. It is evident that the duration and the length of such canard phase depends on how close the phase point was picked up or turns out intermediately to be next to $\mathcal{S}_u$.

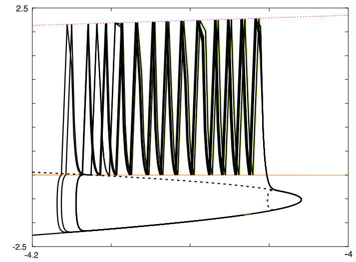

Fig. 7. Canards computed with $\alpha = 6.30749986$ and $\sigma = -0.513045789$. The trajectory follows the unstable manifold $\mathcal{S}_u$ twice: near the original canard and at the end of the burst.

REFERENCES

[1] Arnold, V. I., Afrajmovich, V. S., Ilyashenko, Yu. S., and Shilnikov, L.P. [1994] Bifurcation Theory, *Dynamical Systems V*. Encyclopaedia of Mathematical Sciences (Springer-Verlag).

[2] Belykh, V.N., Belykh, I.V., Colding-Joregensen, M. & Mosekilde, E. [2000] ”Homoclinic bifurcations leading to the emergence of bursting oscillations in cell model,” *Eur. Phys. J.* E **3**, 205-219.

[3] Eckhaus, W. [1983] ”A standard chase on French ducks,” *Lect. Notes in Math.* **985**, 449-494.

[4] Fenichel, N. [1979] ”Geometric singular perturbation theory,” *J. Diff. Eq.* **31** 53-98.

[5] Guckenheimer, J., Hoffman K., and Weckesserand,W. [2000] ”Numerical computations of canards,” *Int. J. Bifurcation and Chaos*, **2**(12), 2669-2689.

[6] Hindmarsh, J.L. & Rose, R.M. [1984] ”A model of neuronal bursting using 3 coupled 1st order differential-equations,” *Proc.R.Soc. London* B **221**(1222), 87-102.

[7] Hodgkin, A.L. & Huxley, A.F. [1952] ”A quantitative description of membrane current and its application to conduction and excitation in nerve,” *J. Physiol.* **117**, 500-544.

[8] Izhikevich, E.M. [2000] ”Neural excitability, spiking and bursting,” *Int. J. Bifurcation and Chaos* **10**(6), 1171-1266.

[9] Marotto, J.R. [1978] ”Snap-back repeller implies chaos in R^n,” *J. Math. Analysis Applic.*, **63**, 199-223.

[10] Mira, C. Gardini, L., Barugola, A. and Cathala, J.-C. [1996] *Chaotic dynamics in two-dimenional noninvertable maps*, World Scientific (Singapore, New Jersey, London).

[11] Rinzel, J. [1987] in *Mathematical Topics in Population Biology, Morphogenesis, and Neurosciences*, edited by E. Teramoto and M. Yamaguti, Lecture Notes in Biomathematics Vol. 71 (Springer, New York), pp. 267-281.

[12] Rulkov, N.F. [2002] ”Modeling of spiking-bursting neural behavior using two-dimensional map,” *Phys. Rev. E* **65** 041922.

[13] Shilnikov, L.P. [1997] ”Mathematical problems of nonlinear dynamics: A Tutorial,” *Int. J. Bifurcation and Chaos*, **7**(9,10), 1953-2003.

[14] Shilnikov, L.P., Shilnikov, A.L., Turaev, D.V. and Chua, L.O. [2001] *Methods of qualitative theory for nonlinear dynamics. Part II*, World Scientific (Singapore, New Jersey, London).